New Understanding of Mercury's Magnetosphere from MESSENGER's First Flyby

James A. Slavin[1]*, Mario H. Acuna[2], Brian J. Anderson[3], Daniel N. Baker[4], Mehdi Benna[2], George Gloeckler[5], Robert E. Gold[3], George C. Ho[3], Rosemary M. Killen[6], Haje Korth[3], Stamatios M. Krimigis[3,7], Ralph L. McNutt, Jr.[3], James M. Raines[5], David Schriver[8], Sean C. Solomon[9], Richard Starr[2], Pavel Travnicek[10], Thomas H. Zurbuchen[6]

[1]Heliophysics Science Division, NASA Goddard Space Flight Center, [2]Solar System Exploration Division, NASA Goddard Space Fight Center, [3]The Johns Hopkins University Applied Physics Laboratory, [4]Laboratory for Atmospheric and Space Physics, University of Colorado, [5]Department of Atmospheric, Oceanic, and Space Sciences, The University of Michigan, [6]Department of Astronomy, University of Maryland, [7]Academy of Athens, Greece, , [9]Institute of Geophysics and Planetary Physics, University of California at Los Angeles, [9]Department of Terrestrial Magnetism, Carnegie Institution of Washington, [10]Astrophysics Institute, Prague

NASA GSFC, Code 670.0, Greenbelt, MD 20771, USA. E-mail:

*Corresponding author contact information: james.a.slavin@nasa.gov; desk phone 301-286-5839; Fax: 301-286-5348.

Observations by the MESSENGER spacecraft on 14 January 2008 have revealed new features of the solar system's smallest planetary magnetosphere. The interplanetary magnetic field orientation was unfavorable for large inputs of energy from the solar wind and no evidence of magnetic substorms, internal magnetic reconnection, or energetic particle acceleration was detected. Large-scale rotations of the magnetic field were measured along the dusk flank of the magnetosphere and ultra-low frequency waves were frequently observed beginning near closest approach. Outbound the spacecraft encountered two current-sheet boundaries across which the magnetic field intensity decreased in a step-like manner. The outer current sheet is the magnetopause boundary. The inner current sheet is similar in structure, but weaker and ~1000 km closer to the planet. Between these two current sheets the magnetic field intensity is depressed by the diamagnetic effect of planetary ions created by the photo-ionization of Mercury's exosphere.

[145 words in abstract] [total word count 2,974]

The MErcury Surface, Space ENvironment, GEochemistry, and Ranging (MESSENGER) spacecraft made the first of three flybys of Mercury on 14 January 2008 (1) and new observations of Mercury's magnetosphere were taken by the Magnetometer (MAG) (2), Energetic Particle and Plasma Spectrometer, which is composed of the Energetic Particle Sensor (EPS) and Fast Imaging Plasma Sensor (FIPS) (3) and X-Ray Spectrometer (XRS) (4) instruments. Companion papers present detailed analyses of the intrinsic planetary magnetic field (5), the composition and intensity of the plasma ion populations (6), and the properties of the neutral exosphere (7). Here we report progress in our understanding of Mercury's magnetosphere that has resulted from the measurements taken during MESSENGER's first flyby.

The intrinsic magnetic field of Mercury was discovered by Mariner 10 during its 1974 and 1975 flybys. A dipole moment of ~ 200 - 350 nT-R_M^3 (8) was determined and found to standoff the typical solar wind at an altitude of ~ 0.5 R_M (1 R_M ~ 2440 km). The interaction of this dipole with the solar wind and embedded interplanetary magnetic field (IMF) produce the magnetosphere. Fig. 1 displays a schematic view of Mercury's magnetosphere derived from the Mariner 10 observations (9) to which new features discovered by MESSENGER have been added.

An overview of the magnetospheric measurements collected by MESSENGER on 14 January 2008 is provided in Fig. 2. The top seven panels show magnetic field components, angular direction, and RMS variation. The eighth panel displays the relative distribution of sodium ion (Na^+) counts measured by FIPS (6). The ninth panel graphs the fluxes of energetic electrons in the 36 to 65 keV energy range measured by EPS. The bottom panel displays count rate from the three gas proportional counters (GPC) of XRS.

The presence of the magnetosphere as an obstacle to the solar wind is signaled by the inbound (not shown) and outbound bow shock (BS) crossings at 18:08:38 and 19:18:55, respectively. Prior to the inbound magnetopause (MP) crossing at 18:42:57 the last extended interval of southward (negative) B_z in the magnetosheath lasted ~ 4 min, ending at 18:38:40. The magnetosheath magnetic field was also observed to be generally

northward following the exit from the magnetosphere at 19:14:15 where the local time was 06:12. A northward IMF is unfavorable to dayside magnetic reconnection with Mercury's magnetic field and greatly limits the rate of solar wind energy transfer across the magnetopause (9). The earlier southward IMF interval(s) prior to MESSENGER's entry into the magnetosphere is expected to have produced strong energetic particle acceleration much as had been observed during Mariner 10's first flyby (9). The lack of measurable energetic electrons within the magnetosphere during MESSENGER's flyby (Fig. 2) indicates that dwell time of energetic electrons and ions (not shown) is less than the ~ 4 min between the end of southward IMF and the entry into the magnetosphere.

MESSENGER observed a well-defined flux transfer event (FTE) between 18:36:21 and 18:36:25 during the inbound magnetosheath passage (Fig 2). FTEs are produced by localized magnetic reconnection between the IMF and the planetary magnetic field at the magnetopause (10). The high time resolution magnetic field data in Fig. 3A shows that this FTE was indeed observed following a brief interval of southward IMF. Its flux rope topology is apparent with the helical magnetic field surrounding and supporting the core region indicated by the bi-polar B_y signatures and the strong core field largely seen in B_z. Given a typical anti-sunward magnetosheath flow speed of ~ 300 km/s and the duration of the event, ~ 4 sec, the size of this MESSENGER FTE is ~1200 km or ~0.5 R_M. Relative to Mercury's magnetosphere, this FTE is ~ 10 times that typically found at the Earth (11). This result supports predictions that finite gyro-radius effects in Mercury's small magnetosphere will lead to relatively large FTEs (12).

The inbound magnetopause crossing into Mercury's magnetotail is identified (Fig. 2) by a rapid transition to a quieter magnetic field directed predominantly northward, but with a longitude angle near 0 degrees, indicating that the spacecraft entered through the dusk flank of the tail into the central plasma sheet (13). The dominance of the B_z component over the B_x and B_y and the sunward longitude angle indicate that MESSENGER was initially located just north of the center of the cross-tail current sheet (Fig. 1). The high ratio of thermal to magnetic pressure typical of this region (13) is evident from the weakness of the magnetic field intensity in Mercury's tail at this point relative to the draped IMF in the adjacent magnetosheath.

Between 18:47 and 18:49 the longitude angle of the magnetic field rotates from 0 deg (i.e. sunward) to near 180 deg (anti-sunward). This change indicates that MESSENGER moved southward through the cross-tail current sheet consistent with its trajectory in Fig. 1. Around 19:00 the spacecraft altitude fell below ~ 800 km and the magnetic field intensity began to increase quickly as MESSENGER moved into the region dominated by Mercury's dipolar planetary magnetic field (5,8). The increase in the magnetic field continued though closest approach and then began to decrease until MESSENGER exited the magnetosphere at 19:14:15 just forward of the dawn terminator at a local time of 06:12.

Examination of the high resolution magnetic field longitude angle in Fig. 3B shows one 360 deg and several 180 deg rotations of the magnetic field in the X-Y plane between 18:43 and 18:46. The durations of the individual rotations ranged from ~ 10 sec to 25 sec. Such rotations of the magnetic field in the Earth's tail near the interface between the flanks of the plasma sheet and the magnetosheath are believed due to hydromagnetic "vortices" driven by the magnetohydrodynamic Kelvin-Helmholtz (K-H) instability with signatures similar to those seen in the MESSENGER observations (14). The twisting of the magnetic field in these vortices can be so severe that these flux tubes disconnect from the magnetosheath, allowing the solar wind plasma they contain to become incorporated into the plasma sheet (15). For these MESSENGER events, the implied scale lengths are ~ 0.6 to 1.5 R_M or ~ 0.4 to 1 times the planetocentric distance to the nose of Mercury's magnetopause. This is smaller than similar features at Earth relative to the dimensions of their respective magnetospheres by a factor of 3 to 8 (14,15).

The FIPS measurements show that Na^+ (Fig. 2) and other ion species (8) throughout the magnetosphere is evident in Fig. 2. The coupling between these photo-ions and the magnetosphere has been the subject of extensive theory and modeling investigations (16,17,18,19) since neutral Na was first detected telescopically from Earth (20). The peaks in Na^+ flux just outside of the inbound and outbound magnetopause crossings (Fig. 2) demonstrate that the neutral sodium atmosphere extends well beyond the magnetosphere where, upon becoming ionized, it is promptly "picked-up" and accelerated by the solar wind. The gyro-radii of Na^+, and the other planetary ions are

expected to be significantly less than the dimensions of the magnetosphere. For this reason the broad maximum in Na^+ ion counts across the nightside magnetosphere (Fig 2) strongly suggests that these ions are becoming assimilated into the plasma sheet and carried sunward by magnetospheric convection. How planetary ions as heavy as Na^+ can be scattered and "thermalized" so that they move with the dominant H^+ ions (6) is not understood (21) and will be the subject of further study. The Na^+ ion counts maximize around closest approach (Fig. 2) and remain high across the dawn magnetosphere due to strong decrease in atmospheric neutral density going from the dayside of the planet into the nightside Na "tail" (7).

During the approach to Mercury there are several intervals where the magnetic field decreased and the RMS variations increased (see horizontal bars in Fig. 2). Such magnetic field variations are generally indicative of the growth of plasma waves stimulated by enhanced plasma density and/or temperature (12). The diamagnetic nature of these decreases is supported by the XRS measurements in that around 19:00 there is an increase in the XRS count rate that closely correlates with the first of these intervals (Fig. 2). The increase in XRS counts seen near 1900 are believed to be due to electron induced fluorescence in the Mg- and Al-filtered GPC and bremsstrahlung in both the Be window of the unfiltered GPC and the Be-Cu collimator in front of all three GPC. The intensity of the signal and the lack of fluorescence in the Cu in the collimator, strongly suggests that the cause is electron flux in the energy range ~1–10 keV. A similar response was seen in the GPC on the NEAR spacecraft during passage through the Earth's radiation belts in January 1998 (23). The presence of enhanced fluxes of 1 – 10 keV electrons is consistent with these night side diamagnetic decreases being due to encounters with regions of enhanced hot plasma density.

The strongest magnetic field decrease occurs following the narrow, magnetopause-like current sheet encountered at 19:10:35 (Fig. 4A). The orientations and thicknesses of this current sheet and the later magnetopause current sheet are very similar. They differ primarily in intensity with the inner current sheet being only about half as strong the magnetopause current sheet. The difference in altitude between these two current sheets is ~ 1000 km. Once again, the enhanced RMS variations in the

magnetic field strongly suggest that this region of decreased magnetic field intensity between these two current sheets is the presence of enhanced plasma pressure.

This "double magnetopause" signature in the MESSENGER magnetic field is a completely new and unexpected feature that has not been observed previously at Mercury or any other planetary magnetospheres. The decrease in the magnetic field in the outer part of the dawn side magnetosphere may be due to the diamagnetic effect of locally created planetary ions and continuously lost to sunward magnetospheric convection. However, it is not apparent how the creation of these pick-up ions would produce the gradients in plasma pressure necessary to support the narrow inner current sheet (Fig. 4A). Alternatively, the inner current sheet could be caused by hot planetary ions that enter the magnetosphere after being picked-up and accelerated by the fast solar wind flow in the magnetosheath. At the dawn terminator the magnetosheath flow speed would typically be ~ 300 km/s. For Na^+, the depth of penetration into the magnetosphere would be ~ 1 gyro-radius or ~ 1000 km, a value comparable to the observed thickness of the region of depressed magnetic field intensity as observed. The thermal temperature of pick-up ions is equal to the speed of the local flow, generally expected to be equal to the **E** x **B** drift speed associated with the cross-magnetosphere potential drop imposed by the solar wind, ~ 10 kV under normal conditions (3). The corresponding convective flow speed is then of order ~ 10 km/s, and planetary ions picked up in the magnetosheath along the flanks of the magnetosphere will have a higher temperature by a factor of order 100 (i.e. $T_i \approx V_{th}^2$) as compared with planetary ions created inside the magnetosphere. Hence, a planetary ion of a given mass accelerated in the magnetosheath will generate ~100 times the thermal pressure of a similar ion picked up in the magnetosphere. Additional observations are necessary to determine if the double magnetopause feature is always present, and how it changes with latitude and longitude over the surface of the magnetosphere, with changing neutral atmosphere densities, and upstream IMF and solar wind conditions. However, as depicted in Fig. 1, the existence of additional magnetopause current sheets may be indicative of the presence of a planetary ion boundary layer(s) to be resolved by future observations.

The ion pick-up process produces distribution functions that are unstable to the growth of ion cyclotron waves and other plasma-wave modes (23). A Na^+ cyclotron

period is ~ 20 sec in Mercury's outer magnetosphere, so during spacecraft flybys the dwell time is marginal for detection of plasma waves generated by heavy planetary ions (21). No clear wave trains near the Na^+ cyclotron frequency are present in the MESSENGER measurements, consistent with Mariner 10 observations (21).

MESSENGER did, however, observe ultra-low frequency (ULF) waves packets with frequencies just below the proton cyclotron frequency (Fig. 4B). They appear similar to the very brief interval of ULF waves observed by Mariner 10 near closest approach during its first encounter (24). However, MESSENGER found these ULF waves to be very common around and following closest approach. These waves often appear as "packets" with amplitudes up to ~ 10 nT peak-to-peak (Fig. 4B). During the outbound portion of the first Mariner 10 flyby these ULF waves may have been masked by the large amplitude fluctuations attributed to substorm activity (9). The third Mariner 10 flyby occurred during northward IMF and experienced relatively calm magnetic fields against which such ULF waves would have been readily observable, but this flyby took place at relatively high latitudes. For these reasons, the MESSENGER and Mariner 10 measurements suggest that these emissions may be confined to the low-latitude magnetosphere.

[Text is 2168 words]

References

1. S.C. Solomon *et al.*: 2001, *Planet. Space Sci.* **49**, 1445-1465 (2001)
2. B.J. Anderson *et al., Space Sci. Rev.,* **131**, 417, doi:10.1007/s11214-007-9246-7 (2007)
3. G.B. Andrews *et al., Space Sci. Rev.,* **131**, 523, doi:10.1007/s11214-007-9272-5 (2007)
4. C.E. Schlemm *et al., Space Sci. Rev.,* **131**, 393, doi:10.1007/s11214-007-9248-5 (2007)
5. B.J. Anderson *et al., this issue* (2008).
6. T. Zurbuchen *et al., this issue* (2008).
7. R.M. Killen *et al., this issue* (2008).
8. J.E.P. Connerney and N.F. Ness, in *Mercury,* pp. 494-513, eds. F. Vilas, C. R. Chapman, and M. S. Matthews (eds.), University of Arizona Press, Tucson (1988).
9. C.T. Russell, D.N. Baker, and J.A. Slavin, in *Mercury,* pp. 514-561, eds. F. Vilas, C. R. Chapman, and M. S. Matthews, University of Arizona Press, Tucson (1988).
10. C.T. Russell and R.C. Elphic, *Space Sci. Rev.,* **22**, 681 (1978)
11. C.T. Russell and R.J. Walker, *J. Geophys. Res.,* **90**, A11, 11,067 (1985).
12. J.A. Slavin *et al., J. Geophys. Res.,* **90**, 10,875 (1985).
13. M.M. Kuznetsova and L.M. Zeleny, Proc. Joint Varenna-Abastumani Int'l School & Workshop on Astrophysics held in Sukhumi, USSR, 19 – 28 May 1986, European Space Agency, SP-251 (1986)
14. D.H. Fairfield *et al., J. Geophys. Res.*, **105**, 21,159, (2000).

15. M. Fujimoto *et al., J. Geophys. Res.*, **103**, 4,391 (1998).
16. W.-H. Ip, *Icarus* **71**, 441 (1987).
17. K. Kabin *et al., Icarus* **143**, 397 (2000)
18. E. Kallio and P. Janhunen, *Annales Geophys.*, **21**, 2,133 (2003)
19. P. Travnicek, P. Hellinger, and D. Schriver, *Geophys. Res. Lett.*, **34**, L05104, doi:10.1029/2007GL028518 (2007).
20. A.E. Potter and T.H. Morgan, *Science*, **229**, 651 (1985).
21. S.A. Boardsen and J.A. Slavin, *Geophys. Res. Lett.*, **34**, L22106, doi:10.1029/2007GL031504 (2007).
22. R. Starr *et al.*, *Adv. Space Res.*, **24,** 1159 (1999)
23. A.L. Brinca and B.T. Tsurutani, *Astron. Astrophys.*, **187**, 311 (1987)
24. C.T. Russell, *Geophys.Res Lett.*, **16**, 1,253 (1989).

Acknowledgements

We thank all of those who have contributed to the success of the first MESSENGER flyby of Mercury. Science discussions with S.A. Boardsen and M. Sarantos and data visualization and graphics support by C. Liebrecht and M. Marosy are gratefully acknowledged.

Figure Legends

Fig. 1. A schematic view of Mercury's magnetosphere high-lighting the new features and phenomena including planetary ion boundary layer, large flux transfer events, flank Kelvin-Helmholtz vortices, and ultra-low frequency plasma waves. The encounter trajectory of the spacecraft is displayed qualitatively.

Fig. 2. Overview of the MESSENGER measurements magnetospheric measurements taken by the magnetometer (MAG), fast ion plasma spectrometer (FIPS), energetic particle spectrometer (EPS), and x-ray Spectrometer (XRS). Closest approach (CA) was at an altitude of 201.5 km at 19:04:39 very near local midnight (00:04 local time). The magnetic field in Mercury Solar Orbital (MSO) coordinates is displayed in the top panels along with the latitude and longitude direction angles and the root-mean-squared (RMS) magnitude calculated over 3 s interval. The MSO coordinate system is defined as X_{MSO} directed from the center of the planet toward the Sun, Z_{MSO} normal to Mercury's orbital plane and positive toward the north celestial pole, and Y_{MSO} positive in the direction opposite to orbital motion. The longitude angle of the magnetic field is defined to be 0 deg toward the Sun increasing in a counter-clockwise looking down from the north celestial pole. The magnetic field latitude is + 90 deg when directed northward and 0 deg when it is in the $X_{MSO} - Y_{MSO}$ plane.

Fig. 3A. MESSENGER magnetic field observations of a large flux transfer event in Mercury's magnetosheath.

Fig. 3B. Magnetic field observations of magnetic field rotations due to Kelvin-Helmholtz driven plasma vortices on the flanks of magnetosphere.

Fig. 4A. Magnetic field observations of the inner current sheet and magnetopause boundaries observed as MESSENGER exited the dawn side magnetosphere near the dawn terminator.

Fig. 4B. Magnetic field observations containing examples of the ULF waves detected in Mercury's magnetosphere.

Fig1

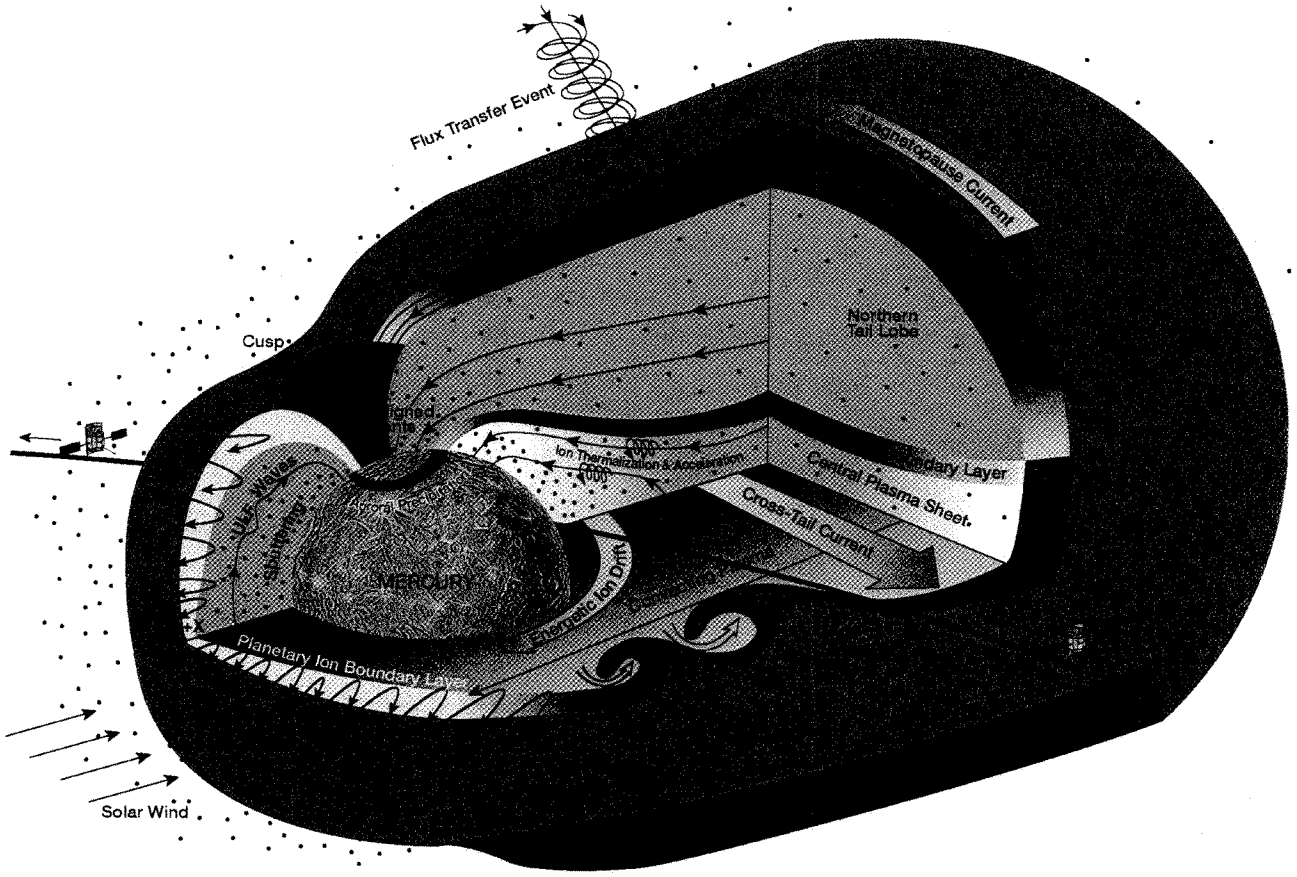
Flux Transfer Event
Magnetopause Current
Cusp
Northern Tail Lobe
Ion Thermalization & Acceleration
Boundary Layer
Central Plasma Sheet
Cross-Tail Current
Alfvén Wings
Shielding
MERCURY
Energetic Ion Drift
Planetary Ion Boundary Layer
Solar Wind

Fig2

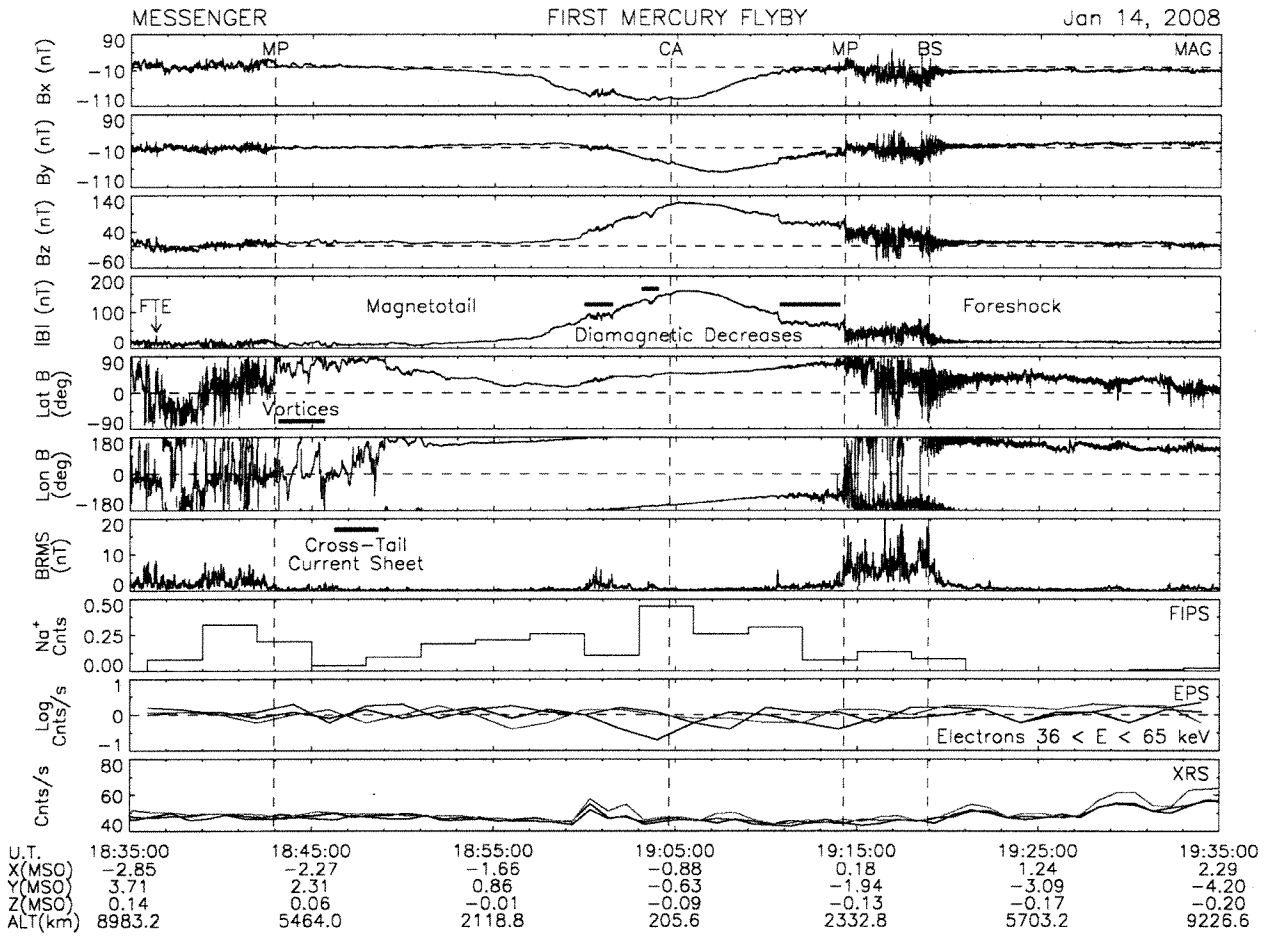
MESSENGER
FIRST MERCURY FLYBY
Jan 14, 2008
MP
CA
MP
BS
MAG
Bx (nT)
By (nT)
Bz (nT)
|B| (nT)
FTE
Magnetotail
Diamagnetic Decreases
Foreshock
Lat B (deg)
Vortices
Lon B (deg)
BRMS (nT)
Cross-Tail Current Sheet
Na+ Cnts
FIPS
Log Cnts/s
EPS
Electrons 36 < E < 65 keV
Cnts/s
XRS
U.T. 18:35:00 18:45:00 18:55:00 19:05:00 19:15:00 19:25:00 19:35:00
X(MSO) −2.85 −2.27 −1.66 −0.88 0.18 1.24 2.29
Y(MSO) 3.71 2.31 0.86 −0.63 −1.94 −3.09 −4.20
Z(MSO) 0.14 0.06 −0.01 −0.09 −0.13 −0.17 −0.20
ALT(km) 8983.2 5464.0 2118.8 205.6 2332.8 5703.2 9226.6

Fig3

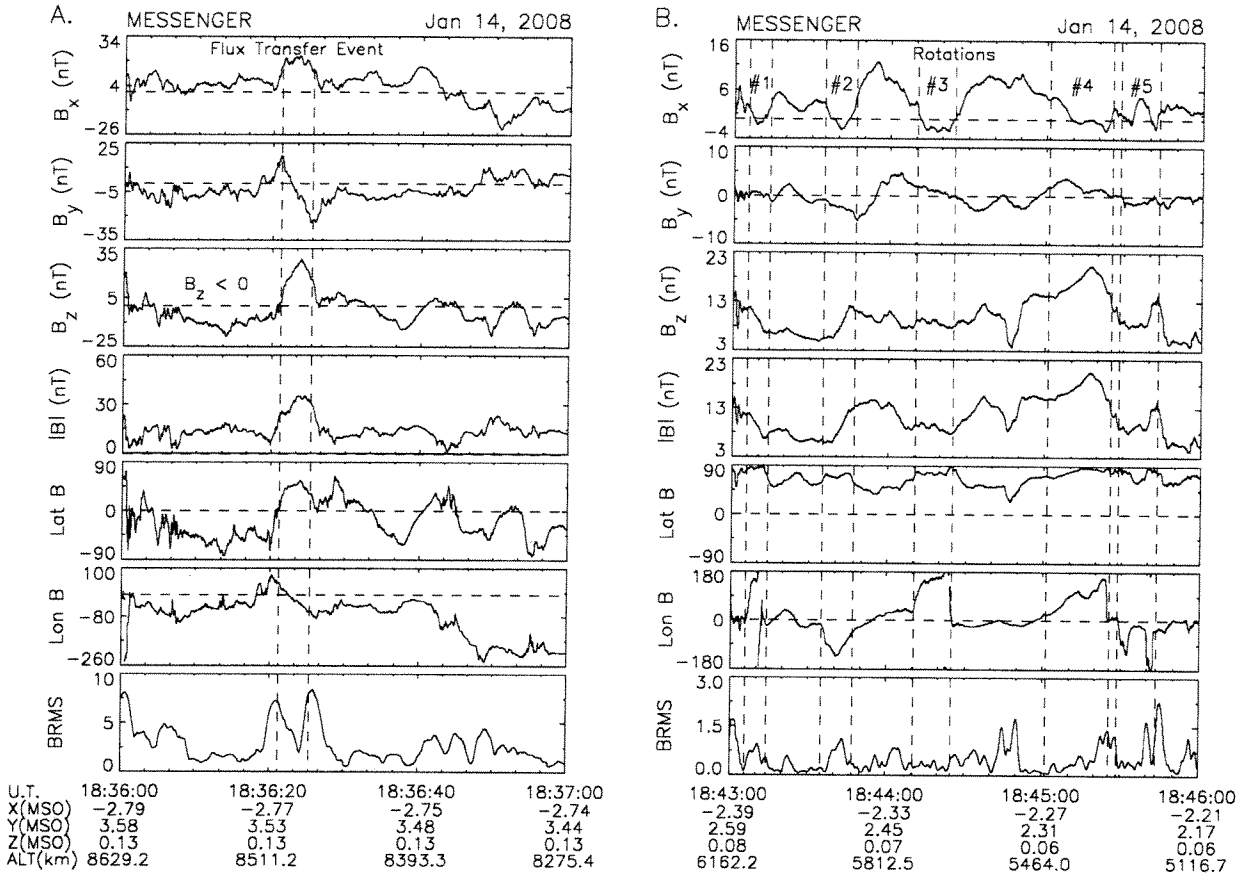
A.
MESSENGER
Jan 14, 2008
Flux Transfer Event
B_z < 0
B_x (nT)
B_y (nT)
B_z (nT)
|B| (nT)
Lat B
Lon B
BRMS
U.T. 18:36:00 18:36:20 18:36:40 18:37:00
X(MSO) −2.79 −2.77 −2.75 −2.74
Y(MSO) 3.58 3.53 3.48 3.44
Z(MSO) 0.13 0.13 0.13 0.13
ALT(km) 8629.2 8511.2 8393.3 8275.4
B.
MESSENGER
Jan 14, 2008
Rotations
#1
#2
#3
#4
#5
B_x (nT)
B_y (nT)
B_z (nT)
|B| (nT)
Lat B
Lon B
BRMS
18:43:00 18:44:00 18:45:00 18:46:00
−2.39 −2.33 −2.27 −2.21
2.59 2.45 2.31 2.17
0.08 0.07 0.06 0.06
6162.2 5812.5 5464.0 5116.7

Fig 4

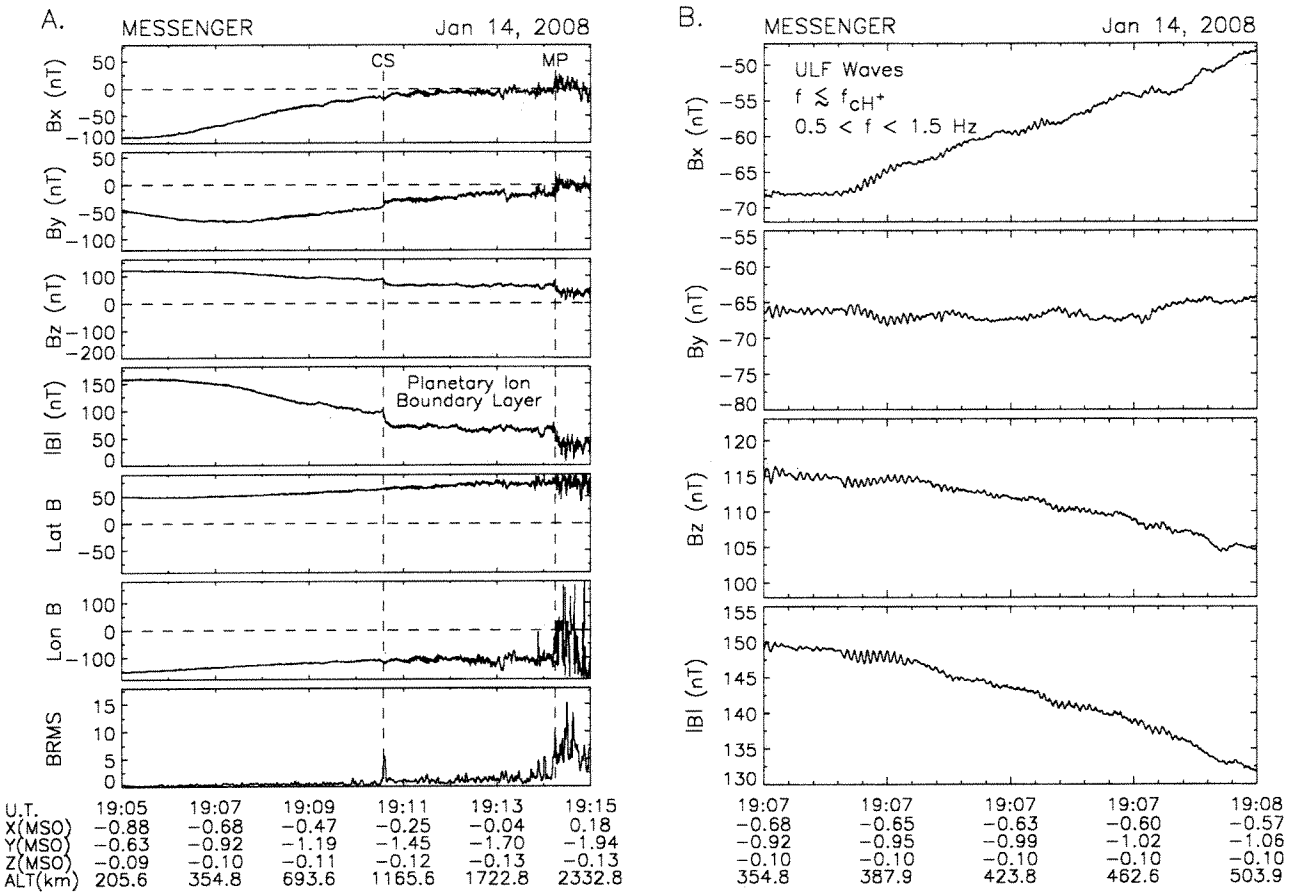
A.
MESSENGER
Jan 14, 2008
CS
MP
Bx (nT)
By (nT)
Bz (nT)
|B| (nT)
Planetary Ion Boundary Layer
Lat B
Lon B
BRMS
U.T. 19:05 19:07 19:09 19:11 19:13 19:15
X(MSO) −0.88 −0.68 −0.47 −0.25 −0.04 0.18
Y(MSO) −0.63 −0.92 −1.19 −1.45 −1.70 −1.94
Z(MSO) −0.09 −0.10 −0.11 −0.12 −0.13 −0.13
ALT(km) 205.6 354.8 693.6 1165.6 1722.8 2332.8
B.
MESSENGER
Jan 14, 2008
ULF Waves
f ≲ fcH+
0.5 < f < 1.5 Hz
Bx (nT)
By (nT)
Bz (nT)
|B| (nT)
19:07 19:07 19:07 19:07 19:08
−0.68 −0.65 −0.63 −0.60 −0.57
−0.92 −0.95 −0.99 −1.02 −1.06
−0.10 −0.10 −0.10 −0.10 −0.10
354.8 387.9 423.8 462.6 503.9